

Nondestructive inspection of crystal defects in LiNbO₃ wafers by using an optical technique

Masayoshi Yamada^{*a}, Masashi Matsumura^a, Masayuki Fukuzawa^a,
Kaoru Higuma^b, and Hirotohi Nagata^b

^aKyoto Institute of Technology,
Department of Electronics and Information Science,
Matsugasaki, Sakyo-ku, Kyoto 606-8585 Japan

^bSumitomo Osaka Cement Co., Ltd.,
Opto-electronics Research Division, New Technology Research Laboratories,
Toyotomi-cho-585, Funabashi-shi, Chiba 274-8601 Japan

ABSTRACT

In order to develop a nondestructive technique for inspection of optical-grade LN wafers used as substrate to fabricate optoelectronic devices such as electro-optic modulator, a scanning infrared polariscope (SIRP), which was developed to measure a small amount of residual strain in optically isotropic GaAs wafers, has been employed. It is demonstrated that the sensitivity of SIRP adopted for LN wafers is high enough to detect the change in refractive index caused by crystal defects, down to the order of 10^{-7} . X-ray topography measurement is also carried out to confirm the usefulness of SIRP as an inspection tool of crystal defects in optical-grade LN wafers.

Keywords: LiNbO₃, defects, birefringence, nondestructive, inspections

1. INTRODUCTION

LiNbO₃ (LN) wafers are widely used as substrate to fabricate optoelectronic devices such as electro-optic (EO) modulator as well as electronic devices such as surface acoustic wave (SAW) filter. The development of the larger size and the higher quality of LN wafers is strongly requested to respond to an increasing demand in optoelectronic and electronic devices. Along with it, a nondestructive inspection technique of LN wafers is also desired to be developed, because the device yield is strongly influenced by the deviation from stoichiometry and the existence of crystal defects in LN wafers.

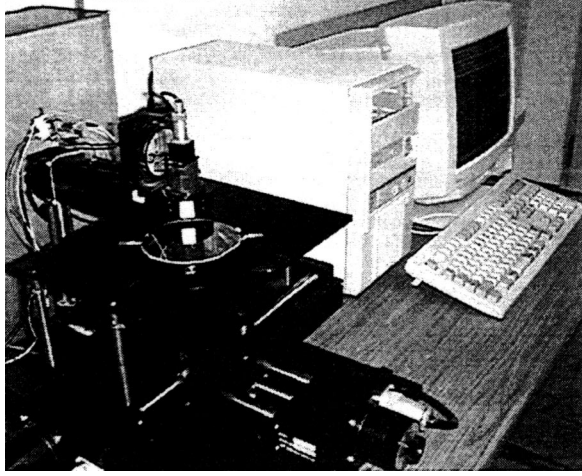
In order to inspect optical-grade LN wafers used in optoelectronic devices, we propose here an optical method using a scanning infrared polariscope (SIRP), with which we can directly measure the change in refractive index, caused by crystal defects, rather than measure crystal defect itself with X-ray topography. The SIRP was developed to measure a small amount of birefringence caused by residual strain in optically isotropic GaAs wafers.¹⁻³ The sensitivity of SIRP was high enough to detect the change in refractive index down to the order of 10^{-7} , caused by undesirable crystal defects in optical-grade LN wafers. We will introduce the SIRP technique for inspecting optical-grade LN wafers currently used for optoelectronic devices, and present the SIRP results, comparing to conventional X-ray topography result.

2. SCANNING INFRARED POLARISCOPE

Picture and schematic diagram of scanning infrared polariscope (SIRP) developed here is shown Fig. 1, in which the principal directions of polarizer and analyzer, and one of the principal axes of birefringence sample to be examined are defined with the angles of ϕ , χ , and ψ , respectively, making to a basal x axis in the measuring coordinate system. The optical configuration is similar to the conventional plane polariscope, except that both polarizer and analyzer are synchronously rotated by an instruction from a computer. A laser diode with the wavelength: $\lambda=1.3 \mu\text{m}$ is used as an incident probing light. In SIRP, we measure the transmitted light intensities of I_{\perp} and I_{\parallel} , as a function of ϕ , under the

*Correspondence: Email: yamada@dj.kit.ac.jp; Telephone: +81-75-724-7422; Fax: +81-75-724-7400

(a) Picture of SIRP



(b) Schematic Diagram

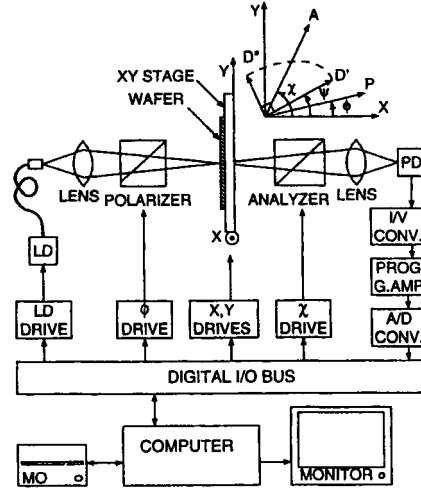


Figure 1. Picture and schematic diagram of scanning infrared polariscopes (SIRP) developed for nondestructive inspection of crystal defects in optical-grade LiNbO_3 wafers. The inset in the schematic diagram shows that the principal directions of polarizer and analyzer, and one of the principal axes of birefringence sample to be examined are defined with the angles of ϕ , χ , and ψ , respectively, making to a basal x axis in the measuring coordinate system.

two conditions for polarizer and analyzer angles; that is, one is the crossed case ($\chi - \phi = \pi / 2$) and the other is the parallel case ($\chi - \phi = 0$) and then calculate the following ratio:

$$I_r(\phi) \equiv \frac{I_{\perp}(\phi)}{I_{\perp}(\phi) + I_{\parallel}(\phi)} = \sin^2 2(\phi - \psi) \sin^2 \left(\frac{\pi d}{\lambda} |\Delta n| \right). \quad (1)$$

Here, $|\Delta n|$ is the difference of refractive index for ordinary and extraordinary light waves propagating through the birefringence sample with the thickness of d . The phase retardation between the ordinary and extraordinary waves becomes $\delta \equiv 2\pi d |\Delta n| / \lambda$. It should be noticed here that the equation for I_r does not include the terms of sample reflectivity as well as light source intensity. By making the sine and cosine transformations for $I_r(\phi)$, we can obtain the following equations:

$$\delta \equiv \frac{2\pi d}{\lambda} |\Delta n| = 2 \arcsin [16(I_{\sin}^2 + I_{\cos}^2)]^{\frac{1}{4}}, \quad \psi = \frac{1}{4} \arctan \frac{I_{\sin}}{I_{\cos}}, \quad (2)$$

in which

$$I_{\sin} \equiv \frac{1}{J} \sum_{j=0}^{J-1} I_r(\phi_j) \sin 4\phi_j, \quad I_{\cos} \equiv \frac{1}{J} \sum_{j=0}^{J-1} I_r(\phi_j) \cos 4\phi_j, \quad (3)$$

where $I_r(\phi_j)$, ($J = 0, \dots, J-1$), is a series of values measured at the interval of $2\pi / J$ for $0 \leq \phi < 2\pi$.

3. EXPERIMENTAL PROCEDURE AND RESULTS

With a newly developed SIRP, we have inspected commercially-available 3-inch and 4-inch diameter optical-grade LN wafers, which are currently used to fabricate optoelectronic devices such as EO modulator. Z-cut wafers were mainly inspected but X-cut wafers were also inspected although the influence of natural birefringence appeared to superimpose on the change in refractive index caused by crystal defects. X-ray topography measurement was carried out in some wafers for comparison with SIRP results.

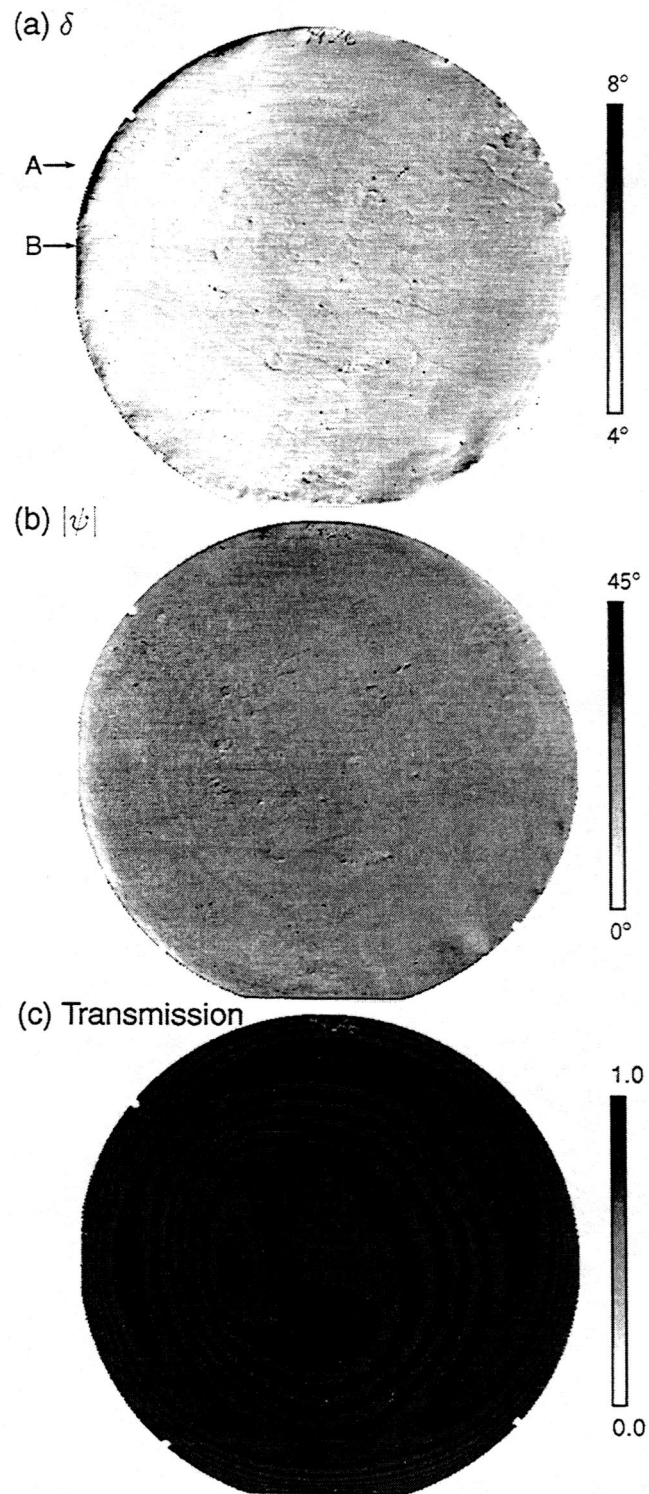


Figure 2. Typical two-dimensional maps of (a) the phase retardation δ , (b) the principal angle ψ of birefringence, and (c) transmission intensity measured in a 4-inch Z-cut optical-grade LN wafer with SIRP.

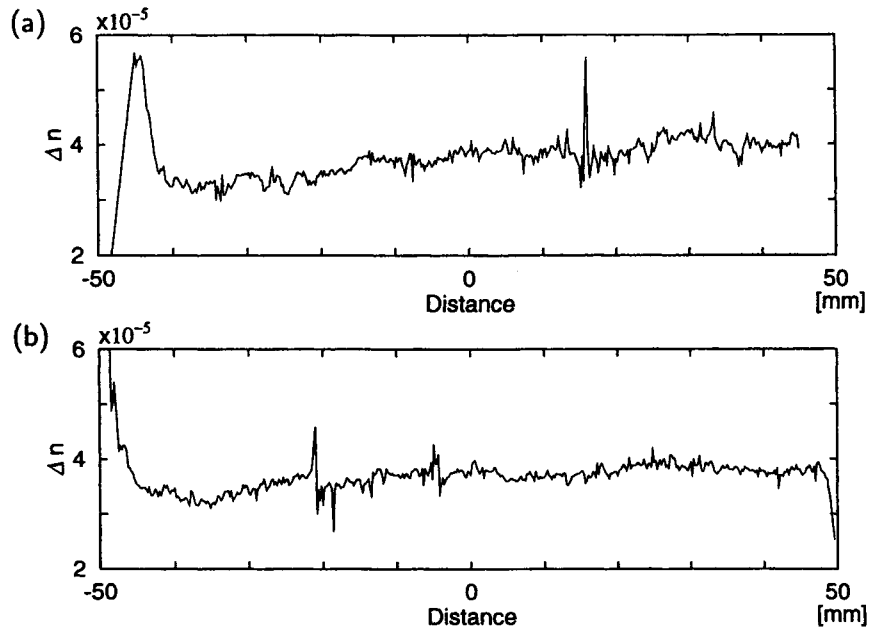


Figure 3. Profiles of $|\Delta n|$ calculated along the lines indicated by the arrows of A and B in Fig. 2 (a).

3.1. Optical inspection with SIRP

Figure 2 shows typical SIRP inspection results made in a 4-inch Z-cut optical-grade LN wafer. SIRP gives us two-dimensional maps of (a) the phase retardation δ , (b) the principal angle ψ of birefringence, and (c) transmission intensity. If the wafer to be inspected has natural birefringence, then the change in refractive index caused by crystal defects may be superimposed on the natural birefringence. In the case of Z-cut LN wafer, we can introduce the probing light almost normal to the wafer surface; that is, almost along the crystallographic z axis and hence the natural birefringence does not so strongly reflect in the δ and ψ maps. On the other hand, in the case of X-cut LN wafer, the natural birefringence strongly appears in their maps. However, the influence of natural birefringence can be reduced by image processings such as subtraction and spatial differentiation. It should be noticed in the map of δ [Fig. 2 (a)] that the subtraction is made by the value corresponding to the natural birefringence.

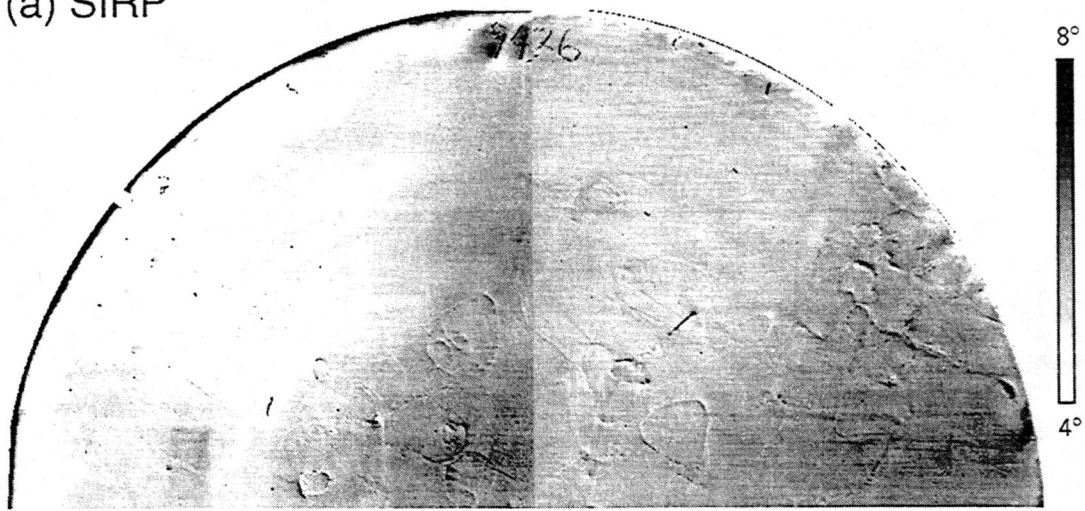
It is clearly seen in the map of δ [Fig. 2 (a)] that spots and crater-like patterns are superimposed on the gradual change in δ from the left hand side to the right hand side. The spots and crater-like patterns are also seen at the same positions in the map of ψ [Fig. 2 (b)]. In addition, an interference pattern is seen in both δ and ψ maps [Fig. 2 (a) and (b)], in coincidence with that seen in the transmission intensity [Fig. 2 (c)], which may be caused by inhomogeneity of wafer thickness.

In order to check the spatial variation of $|\Delta n|$, we have calculated $|\Delta n|$ from the values of δ along the lines indicated by the arrows of A and B in Fig. 2 (a). On the A line, a reasonably large spot defect is laid while on the B line, another spot defect and a crater-like pattern are laid. The profiles of $|\Delta n|$ along the lines of A and B are shown in Fig. 3 (a) and (b). It is found that both spot and crater-like defects cause spike-like changes in $|\Delta n|$, whose peak values attain up to the order of 10^{-5} . It is furthermore found that the SIRP presented here is highly sensitive down to the order of 10^{-7} for the change in refractive index.

3.2. Comparison of SIRP to X-ray topography

Figure 4 shows the comparison of (a) SIRP and (b) X-ray topography results measured in the same wafer shown in Fig. 2. The X-ray topography measurement was made by setting the Burgers vector $[2\bar{1}0]$. It should be noted that the X-ray topography result is influenced by the Burgers vector setting in the measurement. Nevertheless, the spot defects and the crater-like defects seen in the SIRP map can be well corresponded to those in the X-ray topography

(a) SIRP



(b) X-ray topography

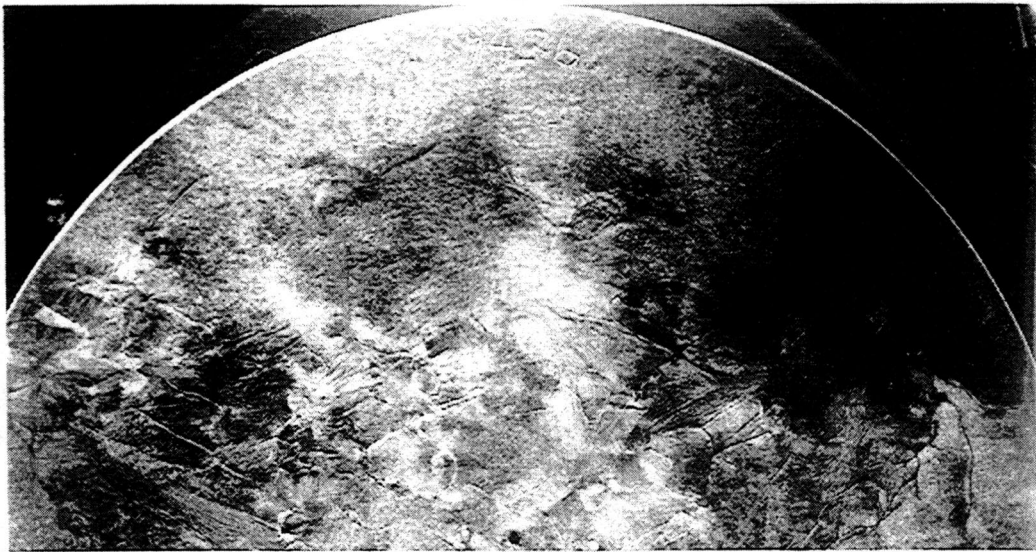


Figure 4. Comparison of (a) SIRP and (b) X-ray topography results measured in a 4-inch Z-cut optical-grade LN wafer.

result. The crater-like defects observed in the SIRP maps are identified mainly due to subgrain boundaries from the X-ray topography result. It is a very interesting result that there are a lot of defects observed near the upper right corner of the SIRP map while there is only a dark region observed in the X-ray topography picture. This can be easily understood from the reason that the X-ray topography is based on the diffraction only from one lattice face relating to Burgers vector. If we make another X-ray topography measurement using a different Burgers vector, then we can observe the defects seen in the upper right corner of the SIRP map.

4. CONCLUDING REMARKS

It is demonstrated that SIRP is a useful inspection tool for optical-grade LN wafers as well as GaAs wafers² used to fabricate optoelectronic devices. The SIRP presented here can detect a small amount of the change in refractive index caused by crystal defects, down to the order of 10^{-7} , and exhibits more clearly crystal defects such as subgrain boundaries than X-ray topography. SAW-grade LN wafers can be easily inspected with the present SIRP instead of the leaky SAW velocity measurement.⁴

ACKNOWLEDGEMENTS

We wish to thank RIGAKU DENKI Co. Ltd. for assistance in X-ray topography measurement. This work has been made in part under a financial support by the Ministry of Education, Science, Sports and Culture (Monbusho).

REFERENCES

1. M. Yamada, "High-sensitivity computer-controlled infrared polariscope," *Rev Sci. Instrum.* **64**, pp. 1815-1821, 1993.
2. M. Yamada, K. Ito, and M. Fukuzawa, "Photoelastic characterization of undoped semi-insulating GaAs wafers with high-spatial-resolution infrared polariscope," in *1996 IEEE Semiconducting and Semi-Insulating Materials Conference*, C. Fontaine, ed., *IEEE* **96CH35881**, pp. 177-180, 1996.
3. M. Fukuzawa and M. Yamada, "Birefringence induced by residual strain in optically isotropic III-V compound crystals," in *Polarization Analysis and Applications to Device Technology*, T. Yoshizawa and H. Yokota, eds., *Proc. SPIE* **2873**, pp. 250-253, 1996.
4. I. Takanaga, J. Hirohashi, and J. Kushibiki, "Homogeneity evaluation of LiNbO₃ and LiTaO₃ single crystals for determining acoustical physical constants," *Jpn. J. Appl. Phys., Part 1* **38**, pp. 3201-3203, 1999.